CONF-970909--4

first draft of paper for *International Symposium on Structural Intermetallics (ISSI-2)*, Seven Springs, Champion PA, Sept. 21-26, 1997, TMS

STABILITY OF ULTRAFINE LAMELLAR STRUCTURES DURING AGING IN TWO-PHASE γ-TiAl ALLOYS

P.J. Maziasz, C.T. Liu, and J.L. Wright
Oak Ridge National Laboratory,
P.O. Box 2008
Oak Ridge, TN 37831-6115

Abstract

Two-phase γ-TiAl alloys such as powder-metallurgy (P/M) Ti-47Al-2Cr-2Nb or Ti-47Al-2Cr-1Nb-Ta hot-extruded above the α-transus temperature (T_α) have unique refined-colony/ultrafine lamellar structures. These lamellar microstructures consist of very fine laths of the γ and α_2 phases, with average interlamellar spacings (λ_L) of 100 nm and α_2-α_2 spacings (λ_α) of 200 nm, and are dominated by γ/α_2 interfaces. This ultrafine lamellar structure remains stable during heat-treatment at 900°C for 2 h, but becomes unstable after 4 h at 982°C. The ultrafine lamellar structure remains relatively stable in both alloys after aging for >5000 h at 800°C, but disappears completely at 1000°C. Continuous coarsening of the lamellar structure begins with the dissolution of fine α_2 lamellea. The aged Ta-modified alloy shows similar lamellar coarsening behavior within the colonies, but has more discontinuous coarsening of the intercolony γ with new precipitation of coarse α_2 and β phase particles. Analytical electron microscopy (AEM) microcompositional data shows that changes in composition of the α_2 phase correlate with microstructural instability.

Introduction

Two-phase γ-TiAl alloys based on Ti-(46-48)Al-2Cr-2Nb (at.%) are being developed and tested for high-temperature structural applications. The properties driving new applications include low density (4 gm/cm^3), and good elevated-temperature strength, stiffness and oxidation-resistance compared to current Ni-based superalloys or titanium alloys [1-9]. However, the mechanical properties of γ-TiAl alloys are extremely sensitive to microstructure, which in turn is also very sensitive to changes in minor alloying elements or in processing parameters. The paradox to date has been trying to achieve a good balance between both room-temperature and high-temperature mechanical properties. Generally, fully-lamellar, coarse-grained alloys have good high-temperature strength and creep-resistance at up to 800°C, but lack room-temperature tensile ductility. By comparison, fine-grained duplex alloys often have better tensile ductility, but have poorer fracture-toughness at room-temperature and lack high-temperature creep-resistance. In 1995, Kim indicated that refined-grained fully-lamellar structures (300 μm grain size, 500 nm lamellar spacing) in an alloy with a composition of Ti-46.5Al-2Cr-3Nb-0.2W (K5) had a significantly better balance of both high-temperature and room-temperature properties [2,10].

In 1995, Liu et al. [11] reported very high levels of room-temperature and high-temperature yield strength (YS) (970 and 850 MPa at 800°C, respectively) in a fully-lamellar powder-metallurgy (P/M) Ti-47Al-2Cr-2Nb alloy with a unique refined colony and ultrafine lamellar structure. This alloy also had 1.4% tensile elongation and 22 MPam$^{1/2}$ fracture toughness at room-temperate. Wang et al. [12] showed that these same unique P/M TiAl alloys also had outstanding creep-resistance at 760°C. Furthermore, in 1996, Liu et al. [13] showed that ingot-metallurgy (I/M) Ti-(46-47)Cr-2Cr-2Nb alloys modified with W and B additions and with somewhat similar fully-lamellar microstructures had YS of 800 MPa with 3-5% tensile ductility and about 30 MPam$^{1/2}$ fracture toughness at room-temperature. Clearly these data indicate that with proper microstructural control, it is possible to have γ-TiAl alloys with balanced good properties.

The purpose of this work is to present more detailed quantitative microstructural and microcompositional data on the fine γ and α_2 components of the ultrafine lamellar structure that initially forms in a P/M Ti-47Al-2Cr-2Nb alloy. The emphasis is on the overall average interlamellar and α_2-α_2 spacings (λ_L and λ_α, resepectively), and on how those parameters change during heat-treatments or long-time aging. High spacial resolution analytical electron microscopy (AEM) data on the compositions of individual phase lamellae or particles are included, to clearly identify phases and to better determine the nature of the processing-induced microstructure. New data on a similar ultrafine lamellar P/M Ti-47Al-2Cr-1Nb-1Ta alloy are also included.

Experimental

The Ti-47Al-2Cr-2Nb (73-1) and Ti-47Al-2Cr-1Nb-1Ta (74-1) -325 mesh alloy powders were produced by Pratt&Whitney (West Palm Beach, FL) using their rotary atomization facility with a helium atmosphere. Wet chemical analysis showed that the powder contained 800 wt. ppm oxygen, 270 wt. ppm carbon and 35 wt. ppm nitrogen. Titanium cans with 15 Kg of powder were extruded at T_1 (below the α-transus temperature) and at T_2 (above the α-transus temperature), and then air cooled. Differential scanning calorimetry data (20°C/min heating, Ar atmosphere) determined the α-transus temperature to be 1320°C. Pieces of the 20 mm diam. extruded rod were heat-treated in vacuum for 1-4 h at 900 to 1350°C and then furnace cooled. Some specimens were then also aged for 72-5020 h at 800 and 1000°C in vacuum. Button-head tensile specimens were electo-discharge machined (EDM) and surface-ground, with the gage axis parallel to the extrusion direction.

Wafers 0.25 mm thick were cut from either the shoulders of tested tensile specimens, or from extruded stock, perpedicular to the extrusion direction. Disks 3 mm diam. were then cut by EDM for transmission electron microscopy (TEM) analysis. TEM specimens were electropolished in a twin-jet unit using a solution of 6% perchloric acid, 60% methanol, 33.5% butyl cellusolve, and 0.5% glycerin at -20°C and 32 V. Conventional TEM was performed on a Philips CM30 (300 KV) microscope. Some electropolished TEM disks were also examined in a Hitachi S4100/FEG scanning electron microscope (SEM).

Lamellar microstructural parameters were measured for most specimens by examining up to three different, representative colonies, and tilting each grain so that the lamellar interfaces were parallel to the electron beam direction (Z) with g at or near <111γ>. Strong diffracting

"The submitted manuscript has been authored by a contractor of the U.S. Government under contract No. DE-AC05-96OR22464. Accordingly, the U.S. Government retains a nonexclusive, royalty-free license to publish or reproduce the published form of this contribution, or allow others to do so, for U.S. Government purposes."

conditions ($s \geq 0$) were used to image all the lamellar interfaces, while weaker diffracting conditions ($s >> 0$) were used to better distinguish the α_2 phase lamellae. Average lamellar spacing (λ_L, including both γ and α_2 lamellae) and α_2-α_2 spacing (λ_α) were measured using a line-intercept method with >100 lamellae in the field of view. Several of the largest and smallest of each lamellar phase constituent in each analyzed area/colony were also measured to establish the maximum representative size range.

Microcompositional analysis of individual phase lamellae within colonies of selected specimens was performed using X-ray energy dispersive spectroscopy (XEDS) on either a Philips 400T (100 KV) or a CM200 (200 KV) analytical electron microscope (AEM) equipped with a field-emission gun (FEG, probe-size: 2-5 nm). XEDS analysis of coarser intercolony phase consituents was done on a Philips CM12 (LaB_6, 120KV). XEDS were quantified using a standardless method, but *k*-factors for aluminum were checked against a known standard, as recommended by Ramanujan et al. [14,15].

Results

As-Extruded Ultrafine Lamellar Microstructures

P/M 73-1 alloy consolidated by hot-extrusion at temperature T_1 well below the α-transus temperature (T_α) had a very fine-grained (<1 µm), duplex structure, but poor mechanical properties at elevated temperatures [11], so further analysis was not done. The same P/M alloy consolidated by extrusion at T_2 above T_α was fully-dense with a near-fully lamellar structure (Fig. 1). The lamellar structure consists of a unique combination of refined colony size (70 µm) with very little intercolony γ (1-3 µm thick, < 5 vol.%) [11], and an ultrafine lamellar structure within the colonies. The P/M 74-1 alloy extruded at T_2 had a similar microstructure, but with a slighlty smaller colony size and even less intercolony γ. Quantitative lamellar microstructural data are given in Table 1.

The as-extruded ultrafine lamellar structure of P/M 73-1 alloy consists of very uniformly spaced, alternating lamellae of the γ and α_2 phases (Figs. 1-3). The overall λ_L is about 100 nm and λ_a is 220 nm. The γ lamellae are typically 100-200 nm wide (Fig. 2a), but a few can be as wide as 500 nm and contain twin subboundaries. The α_2 lamellae are much thinner (20-76 nm). This ultrafine lamellar structure is dominated by γ/α_2 boundaries with few γ/γ twins. The ultrafine γ and α_2 lamellae all have the same characteristic $(111)\gamma // (0001)\alpha_2$ and $<110>\gamma // <1120>\alpha_2$ crystallographic habit relationship between close-packed planes and directions in those respective phases seen by others in coarser lamellar structures [9]. It is particularly noteworthy that these ultrafine lamellae are very straight across the length of the colonies, and free of the common structural imperfections (kinks, jogs, subboundaries, etc.) found in lamellar structures by others [15].

The Ta-modified 74-1 alloy has a slightly finer initial lamellar structure with smaller λ_L (Table 1), which is due to a few more γ/γ twins within the wider γ lamellae. The λ_α remains 220 nm. All other features and characteristics are the same as found in the unmodified P/M Ti-47Al-2Cr-2Nb alloy.

Heat-Treatment Affects on the Ultrafine Lamellar Structure

Heat-treatments of 4 h at 982°C with or without an additional 8 h at 704°C (to stabilize and stress-relieve the material, respectively) were found to slightly degrade the as-extruded microstructure of the 73-1 alloy. The ultrafine lamellar showed subtle signs of the early stages of continuous lamellar coarsening, including measureable increases in both λ_L and λ_α (Table 1), as well as partial dissolution of the initially continuous α_2 lamellae. Consistently, the colony boundaries also show evidence of discontinuous coarsening, which increases the amount of intercolony γ and causes coarse α_2 precipitation at the expense of the adjacent lamellar structure (Fig. 4). By contrast, heat-treatment for 2 h at 900°C produces no discernable changes in the as-extruded intercolony γ or ultrafine lamellar structures (Table 1). This heat-treatment appeared to optimize room-temperature tensile properties for both P/M 73-1 and 74-1 alloys [11,16] and was therefore chosen as the "standard" stress-relief treatment for subsequent mechanical properties studies of P/M and I/M ultrafine lamellar TiAl alloys [13,16,18].

To complete studies on the formation and stability of these refined-colony/ultrafine-lamellar alloys, as-extruded P/M 73-1 material was heat-treated for 2 h at up to 1350°C [11]. Heat-treatment at 1320°C (almost exactly at T_α) did not change the colony size, but dramatically coarsened the lamellar structure (both λ_L and λ_α increase by a factor of 4) (Table 1 and Fig. 5). Conversely, heat-treatment at 1350°C (above T_α) greatly increases the colony size, but has only a small effect on the ultrafine lamellar structure (Table 1). The P/M 74-1 alloy showed very similar behavior.

Aging Affects on the Ultrafine Lamellar Structure

Specimens of the as-extruded P/M Ti-47Al-2Cr-2Nb alloy (+2 h at 900°C) were aged at 800 and 1000°C for times ranging from 72 to 5040 h. Aging at 800°C for <2160 h produced no noticeable changes in the initial lamellar structure detectable by optical and TEM microstructural examination [16]. Aging for 5040 h at 800°C still shows very little change optically (Fig. 6a and 6b), but SEM (Fig. 7a) and TEM (Figs 2,3, and 8a) analyses do reveal subtle changes in both the intercolony and lamellar components of the structure. Discontinuous coarsening slightly increases the thickness of the intercolony γ and causes some new, coarse intercolony α_2 particles to form (compare Figs 1 and 7a and 8a). The lamellar structure also shows subtle changes which indicate that the very early stages of continuous lamellar coarsening are occurring. While there is very little change in λ_L (Table 1 and Fig. 2), there is a measureable change in λ_α and observable fragmenting and thinning of the α_2 lamellae that is consistent with dissolution (Fig. 3). Other work on aging and coarsening of similar ultrafine lamellar structures has shown that dissolution of the α_2 lamellae is the first step in the continuous coarsening of the overall lamellar structure [17].

The effects of aging for 5040 h at 800 and 1000°C on the ultrafine lamellar structure of the P/M Ti-47Al-2Cr-1Nb-Ta alloy are similar to those seen in the Ta-free alloy, but there are minor differences. At 800°C, the 74-1 alloy has slightly more discontinous coarsening of the intercolony boundary regions, with considerably more precipitation of coarse α_2 particles along the interfaces between the intercolony γ and the lamellar structures (Figs. 7b and 8b). Within the lamellar colonies, the increases in both λ_L and λ_α in the Ta-modified 74-1 alloy are similar to those observed in the 73-1 base alloy (Table 1).

XEDS Microcompositional Phase Analysis in As-Extruded, Heat-Treated or Aged Ultrafine Lamellar Structures

XEDS analysis of the composition of coarser individual phase particles within the intercolony γ regions were performed using a Philips CM12 (120KV, LaB_6, 100-200 nm probe) AEM. High-spacial resolution XEDS of individual γ and α_2 lamellae were measured using a Philips EM400T (100KV, FEG, <5 nm probe) or a CM200 (200KV, FEG, < 2nm probe) AEMs. Average values of individual measurements of the two phases in various alloys are given in Table 2.

The initial microstructure (as-extruded + heat-treated 2 h at 900°C) of the 73-1 alloy shows about 39 at.% Al and more Cr (1.5-2.0 enrichment) in both lamellar and intercolony α_2 relative to adjacent γ. AEM results on the initial structure of the 74-1 alloy are similar. Partitioning of Nb and/or Ta is also fairly even between the two phases.

AEM was performed on specimens of both 73-1 and 74-1 heat-treated for 4 h at 982°C to clearly identify the new coarse precipitate particles that formed in the intercolony region of the microstructure. In both cases, the new precipitate particles were all α_2 phase (no β), but there is a significant difference in composition between these new precipitates that form during discontinuous coarsening and those found in the initial microstructure. The α_2 particles produced during heat-treatment have less aluminum than those found in the initial microstructure (34-35 at.% compared to 39-40%), and no longer show any chromium enrichment.

Finally, AEM measurements of both intercolony and lamellar phase constituents in the 73-1 alloy aged 5040 h at 800°C show even larger composition differences between the γ and α_2 phases relative to the initial microstructure (Table 2). Both lamellar and intercolony α_2 have even less Al (31-32 at.%) after long-term aging, and now also have less Cr and Nb than the γ.

Discussion

These unique refined-colony/ultrafine lamellar microstructures are new and interesting, but they are important because they produce an outstanding balance of mechanical properties in these two-phase γ-TiAl alloys at room- and elevated-temperatures [11,13,16,17]. The P/M Ti-47Al-2Cr-2Nb alloy (extruded at T_2 and heat-treated at 900°C) has 1.4% total tensile elongation, YS of 970 MPa, and a fracture toughness of 22 MPam$^{1/2}$, all at room-temperature [11]. Heat-treatment of the P/M alloy at 1320°C increases the elongation to 3.6%, but lowers the YS to 650 MPa [16]. Liu et al. [16,17] attributes the improved ductility in these P/M γ-TiAl alloys mainly to their refined colony size. Kim [2] noted a similar relationship between colony size and ductility for the FL I/M K5 (Ti-46.5Al-2Cr-3Nb-0.2W) alloy, with colony sizes in the 100-300 μm range and elongations in the 2-4% range. Liu et al. [11] explains the very high strength of this P/M material on the basis of the ultrafine lamellar structure, comparing strengthened by the ultrafine and regularly alternating γ and α_2 platelets as similar to a micro-laminate. Even more important than the room-temperature strength is the strength that these ultrafine lamellar alloys retain at high temperatures. These P/M Ti-47Al-2Cr-2Nb alloys have a YS of over 800 MPa at 800°C [11].

In terms of their formation, these P/M Ti-47Al-2Cr-2Nb and Ti-47Al-2Cr-1Nb-1Ta alloys appear to fall into catagory of Type I fully-lamellar microstructures described by Kim [18]. Such microstructures are formed by heating or processing the TiAl alloy above Tα, and then the γ lamellae nucleate in the α-grains as the alloy is undercooled. Generally, increasing the cooling rate (larger undercooling) decreases λ_L until a massive transformation of α to γ occurs, preventing the formation of the fully-lamellar structure [18-20]. The residual disordered α phase trapped between the γ lamellae then transforms to α_2 below the eutectoid temperature to produce the final lamellar microstructure. For binary TiAl alloys, such fully-lamellar structures form more readily in Ti-47Al alloys than in alloys with less Al, and are also more resistant to discontinuous coarsening during aging [21]. Generally, slow furnace cooling rates produce λ_L of 1 μm or more in binary TiAl alloys, and polysynthetically twinned TiAl crystals have lamellar structures with λ_L slightly less than 1-2 μm and λ_α of 5-10 μm, dominated by γ/γ interfaces [8, 19-22]. Kim [19] has reported an ultrafine lamellar structure with λ_L of 0.03-0.2 μm in a Ti-47Al-1Cr-1V-2.5Mo alloy heat-treated above Tα, and Soe et al. [24] report λ_L of 0.3 μm and λ_α of about 1 μm in investment-cast Ti-47Al-2Nb-2Mn with 0.8 % TiB_2, but generally there are no systematic studies of comparable alloys with fully-lamellar structures consistently as fine as reported here.

The ultrafine lamellar microstructure forms easily in the P/M Ti-47Al-2Cr-2Nb alloy processed above Tα. At the same processing conditions (extrusion temperature and cooling rate), alloying changes of reduced Nb and added Ta slightly refine λ_L and almost eliminate the intercolony γ. Maziasz et al. [18,25] have found that additions of B+W to I/M Ti-47Al or Ti-47Al-2Cr-2Nb alloys also refine both λ_L and λ_α . Rejection of W by the γ lamellae as they form which retards their growth has been suggested as the reason for this effect [14,18,25], and is consistent with the γ/α_2 interfacial W segregation observed by Larson et al. [26], and the W partitioning to the α_2 lamellae observed by XEDS [27]. A comparison of the α_2 phase composition in the initial and in the heat-treated or the aged specimens of the Ti-47Al-2Cr-2Nb alloy would suggest that Cr and Nb behave analogous to W, and also are dissolved by the metastable α phase as they are rejected by growing γ lamellae.

The ultrafine lamellar structure that forms during cooling of the as-processed material must also remain stable during subsequent heat-treatment and thermal aging to provide technologically relevent improvements in high-temperature strength. In fact it is somewhat of a paradox for finer lamellar structures to also be more stable, because reducing the surface area of the structure is one of the driving forces for continuous lamellar coarsening [22]. The most important factors governing the stability and coarsening resistance of these ultrafine lamellar structures at high-temperatures appear to be the resistance of the original fine α_2 lamellae to dissolution and their metastable composition. Clearly, this structure is unstable in the P/M Ti-47Al-2Cr-2Nb alloy during heat-treatment or aging near or at 1000°C. The compositional change in the intercolony α_2 that precipitates after 4 h at 982°C is consistent with the equilibrium α_2 phase composition at that temperature (less Al). Aging for 5040 h at 800°C produces only subtle microstructural changes, consistent with the kinetics of diffusion being much more sluggish at the lower aging temperature, and the equilibrium α_2 phase composition being even lower in aluminum (approaching Ti-25Al). However, despite such small degree of microstructural coarsening, there is a much larger change in the composition of the α_2 phase, which is the same in the thin, lamellae that are dissolving from the original structure and the new α_2 particles that have formed during aging in the intercolony γ (Table 2). These data clearly indicate that diffusion is moving the originally metastable α_2 lamellae toward their equilibrium phase composition, and that such changes, include repartitioning of Cr and Nb back into the γ phase, precede dissolution.

Similar arguements have been offered to explain the improved aging resistance of the W+B modified simpler Ti-47Al alloys. Tungsten is also forced into the metastable a_2 lamellae when they form, and apparently is repartitioning much more slowly during aging at 1000°C than the Al [14,18]. Segregation of elements like W, Cr, Nb and Ta to the fine, metastable α_2 lamellae would then explain how those elements enable the ultrafine lamellar structure to form in the first place. The need for those elements to diffuse out of the metastable α_2 lamellae before they can dissolve at lower temperatures would then explain why those particular elements increase the coarsening resistance (at least relative to binary alloys) of such structures during aging. The reason for Cr and Nb dissolving in the metastable α_2 lamellae at higher temperatures initially but then being rejected at lower temperatures is not as clear; it may reflect solubility differences between disorderd α and ordered α_2 for those elements. However, it is clear that the longer the α_2 lamellae resists dissolution during aging, the longer the ultrafine lamellar structure remains stable and resists continuous coarsening. While λ_L may be the primary strength-controlling factor at any point in time, the role of the α_2 lamellae seems to be to act as the "glue" that holds these ultrafine lamellae together at high temperatures.

In summary, achieving refined-colony/ultrafine-lamellar produces a combination of ductility and strength at room-temperature and strength at high-temperatures that has not been achieved previously in fully-lamellar two-phase γ-TiAl alloys. The refined colony size makes these alloys ductile, while the ultrafine λ_L makes them strong. Data presented here showing lamellar stability and microcompositional evolution during heat-treatment or aging, demonstrate that controlling and stabilizing the lamallar structure in general, and the fine α_2 component in particular, is a very important part of any alloy design strategy aimed at improving the properties of γ-TiAl alloys.

Conclusions

1. Hot-extrusion of P/M Ti-47Al-2Cr-2Nb and Ti-47Al-2Cr-1Nb-1Ta alloys at T_2 above T_α produces ultrafine lamellar structures ($\lambda_L \leq 100$ nm and $\lambda_\alpha \leq 220$ nm) with a refined colony size ≤ 70 nm.

2. Such microstructures do not change after a heat-treatment of 2h at 900°C, but do show early stages of continuous lamellar coarsening after 4 h at 982°C. Heat-treatment for 2 h at 1320°C coarsens λ_L and λ_α considerably with little change in colony size, while 2 h at 1350°C dramatically increases the colony size with little change in λ_L and λ_α.

3. Aging for 5040 h at 1000°C totally coarsens the initial ultrafine lamellar structure in both 73-1 and 74-1 alloys, whereas similar aging at 800°C produces little change. Both alloys show the very earliest stages (α_2 dissolution) of continuous lamellar coarsening. The Ta-modified 74-1 alloy appears to show more discontinuous coarsening at intercolony boundaries, with more precipitation of coarse α_2 particles.

4. AEM studies of microcomposition of individual lamellae and phase particles show that α_2 phase in the initial microstructure contains about 40 at.% Al and more Cr than adjacent γ lamellae. Both heat-treatments near 1000°C and long-term aging at 800°C show compositional changes in the α_2 lamellae (much less Al, and less Cr and Nb), which indicate that the initial lamellae form with a metastable composition, and diffusion toward the equilibrium phase composition precedes dissolution of those lamellae.

ACKNOWLEDGEMENTS

Thanks to D.S. Easton and L. Heatherly for alloy preparation and fabrication. Thanks to J.W. Jones for preparing specimens for electron microscopy. Thanks to D. Clemens at Pratt&Whitney, Advanced Engineering Operations, West Palm Beach, FL, for producing TiAl powders and support of the CRADA work. Thanks to P. Angelini for program management support for both the DP-CRADA and the Advanced Industrial Materials (AIM) work. Thanks to L. Heatherly and D.S. Easton for reviewing the manuscript. Research sponsored by the U.S. Department of Energy, Assistant Secretary for Energy Efficiency and Renewable Energy, Office of Industrial Technologies, AIM Program, and Assistant Secretary of Defense Programs (DP), Technology Management Group, Technology Transfer Initiative, under contract DE-AC05-96OR22464 with Lockheed-Martin Energy Research Corp.

REFERENCES

1. Y-W. Kim, JOM, 46 (1994) 30-40.
2. Y-W. Kim, in Gamma Titanium Aluminides, eds. Y-W. Kim, R. Wagner, M. Yamaguchi (Warrendale, PA: TMS, 1995) 637-654.
3. Y-W. Kim: in High-Temperature Ordered Intermetallics Alloys IV, vol. 213, eds. L.A. Johnson, D.P. Pope and J.O. Stiegler (Pittsburgh, PA: MRS, 1991) 777-794.
4. D.M. Dimiduk, in Gamma Titanium Aluminides, eds. Y-W. Kim, R. Wagner, M. Yamaguchi (Warrendale, PA: TMS, 1995) 3-20.
5. C.M. Austin and T.J. Kelly, in Gamma Titanium Aluminides, eds. Y-W. Kim, R. Wagner, M. Yamaguchi (Warrendale, PA: TMS, 1995) 21-40.
6. R. Wagner, et al., in Gamma Titanium Aluminides, eds. Y-W. Kim, R. Wagner, M. Yamaguchi (Warrendale, PA: TMS, 1995) 387-404.
7. S. Huang, in Structural Intermetallics, eds. R. Darolia, et al. (Warrendale, PA: TMS, 1993) 299-307.
8. M. Yamaguchi and H. Inui, in Structural Intermetallics, eds. R. Darolia, et al. (Warrendale, PA: TMS, 1993) 127-142.
9. M. Yamaguchi and Y. Umakoshi, Prog. Mater. Sci. Eng., 34 (1) (1990) 1-148.
10. J. Kumpfert, Y-W. Kim and D.M. Dimiduk, Mater. Sci. and Engin., A192/193 (1995) 465-473.
11. C.T. Liu, et al., in Gamma Titanium Aluminides, eds. Y-W. Kim, R. Wagner, M. Yamaguchi (Warrendale, PA: TMS, 1995), 679-688.
12. J.N. Wang, et al., in Gamma Titanium Aluminides, eds. Y-W. Kim, R. Wagner, M. Yamaguchi (Warrendale, PA: TMS, 1995), 949-957.
13. C.T. Liu, et al., Intermetallics, 4 (1996) 429-440.
14. R.V. Ramanujan, P.J. Maziasz and C.T. Liu, Acta Mater., 44 (7) (1996) 2611-2642.
15. R.V. Ramanujan and P.J. Maziasz, Met. and Mater. Trans. A, 27A (1996) 1661-1673.
16. C.T. Liu and P.J, Maziasz, unpublished data, ORNL, 1995, presented at Symposium on Intermetallic Compounds at the JIM '95 Meeting, December 13-15, 1995 in Honolulu, HA.
17.C.T. Liu, P.J. Maziasz and J.L. Wright, "Key Microstructures Controlling the Mechanical Properties of Two-Phase TiAl Alloys With Lamellar Structures," to be published in Proc. Symp. High-Temperature Ordered Intermetallic Alloys VII, MRS, Pittsburgh, PA in 1997.
18. P.J. Maziasz, et al., Intermetallics, 5 (1997) 83-95.
19. Y-W. Kim; Acta Metall. et Mater., 40 (1992) 1121-1134.
20. M. Takeyama, T. Kumagai, N. Nakamura, M. Kikuchi; in Structural Intermetallics, eds. R. Darolia, J. Lewandowski, C.T. Liu, P. Martin, D. Miracle and M. Nathal (Warrendale, PA: TMS, 1993) 167-176.
21. P. Wang and V.J. Vasudevan; High Temperature Ordered Intermetallics V, ed. I. Baker, R. Darolia, J.D. Wittenberger, and M.H. Yoo, vol. 288 (Pittsburgh, PA: MRS, 1993) 229-236.
22. J.D. Livingston and J.W. Cahn; Acta Met. 22 (1974) 495-503.
23. Y. Umakoshi, T. Nakano, and T. Yamane; Matls. Sci. and Engin. A152 (1992) 81-88.
24. D.Y. Seo, T.R. Bieler and D.E. Larson, "Effect of Interstitial Concentration and Heat Treatment on Microstructure and Primary Creep of Investment Cast Ti-47Al-2Nb-2Mn with 0.8 v.% TiB_2," to be published in Proc. Symp. High-Temperature Ordered Intermetallic Alloys VII, MRS, Pittsburgh, PA in 1997.
25. P.J. Maziasz and C.T. Liu, "Ultrafine Fully-Lamellar Structures in Two-Phase γ-TiAl Alloys," to be published in Proc. Symp. High-Temperature Ordered Intermetallic Alloys VII, (Pittsburgh, PA: MRS) in 1997.
26. D.J. Larson, C.T. Liu and M.K. Miller, "Microstructural Characterization of Segregation and Precipitation in α_2+γ Titanium Aluminides;" submitted to Matls. Sci. and Engin. in 1997.
27. P.J. Maziasz and C.T. Liu, "Development of Ultrafine Lamellar Structures in Two-Phase γ-TiAl Alloys;" submitted to Met. and Matls. Trans. A in 1997.

FIGURE CAPTIONS

Fig. 1 - a.) SEM (electropolished surface) and b.) TEM of P/M Ti-47Al-2Cr-2Nb (73-1) hot-extruded at T_2 above T_α to produce a refined-colony, ultrafine lamellar structure.

Fig. 2 - TEM of P/M Ti-47Al-2Cr-2Nb (73-1) a.) as-hot-extruded (T_2) and heat-treated for 2 h at 900°C, and b.) aged for 5040 h at 800°C at lower magnification, showing the typical very straight and evenly spaced ultrafine lamellar structure found within each colony.

Fig. 3 - TEM of P/M Ti-47Al-2Cr-2Nb (73-1) a.) as-hot-extruded (T_2) and heat-treated for 2 h at 900°C, and b.) aged for 5040 h at 800°C at higher magnification, showing the finer α_2 lamellae found uniformly distributed between most larger γ lamellae. b.) shows dissolution of the α_2 lamellae that is the first step in continuous coarsening of the such lamellar structures.

Fig. 4 - TEM showing the discontinuous coarsening that occurs along the intercolony boundaries during heat-treatment at 982°C for 4 h of P/M Ti-47Al-2Cr-2Nb (73-1) hot-extruded at T_2.

Fig. 5 - SEM (electropolished surface) showing the effects of heat-treatments of a.) 2h at 1320°C and b.) 2h at 1350°C on the lamellar and colony structures of P/M Ti-47Al-2Cr-2Nb (73-1) hot-extruded at T_2.

Fig. 6 - Optical (polished and etched) micrographs of P/M Ti-47Al-2Cr-2Nb (73-1) hot-extruded at T_2, showing a.) initial microstructure (with heat-treatment of 2 h at 900°C), b.) aged 5040 h at 800°C, and c.) aged 5040 h at 1000°C. Continuous and discontinuous coarsening complete remove the ultrafine lamellar structure during aging at 1000°C.

Fig. 7 - SEM (electropolished surface) of TEM disks showing the difference in discontinuous coarsening at intercolony boundaries of a.) P/M Ti-47Al-2Cr-2Nb (73-1) and b.) P/M Ti-47Al-2Cr-1Nb-1Ta (74-1) alloys aged for 5040 h at 800°C.

Fig. 8 - TEM showing the difference in discontinuous coarsening at intercolony boundaries of a.) P/M Ti-47Al-2Cr-2Nb (73-1) and b.) P/M Ti-47Al-2Cr-1Nb-1Ta (74-1) alloys aged for 5040 h at 800°C.

Table 1 - Quantitative Lamellar Microstructural Data on Hot-Extruded Above T_α and Heat-Treated P/M Ti-47Al-2Cr-2Nb and P/M Ti-47Al-2Cr-1Nb-1Ta Alloys

Heat-Treatment	Interlamellar spacing (nm)	α_2-α_2 spacing (nm)	γ-width (nm)	α_2-width (nm)
		P/M Ti-47Al-2Cr-2Nb		
none	100	220	100-500	20-76
2 h at 900°C	similar to above			
4 h at 982°C	180	325	60-600	20-60
2 h at 1320°C	390 (±75)	900 (±300)	80-2000	70-400
2 h at 1350°C	140	300	50-300	70-430
2 h at 900°C + aged >5000 h at 800°C	120	285	70-630	15-45
		P/M Ti-47Al-2Cr-1Nb-1Ta		
none	86	220	40-480	13-76
2 h at 900°C	similar to above			
2 h at 900°C + aged >5000 h at 800°C	114	275	80-480	14-72

Table 2 - Quantitative Microcompositional Analysis of Phases in P/M Ti-47Al-2Cr-2Nb and P/M Ti-47Al-2Cr-1Nb-1Ta Alloys

Extrusion/Heat-Treatment	Phase	Composition (at.%) Al	Ti	Cr	Nb	Ta
		P/M Ti-47Al-2Cr-2Nb				
T_2/ 2 h at 900°C	lamellar γ (8)[a]	47.4	49.2	1.6	1.8	
	lamellar α_2 (4)	39	56	3	1.7	
	equiaxed γ (1)	46.4	50	1.6	2.0	
	intercolony γ (9)	49	47.3	1.4	2.3	
	intercolony α_2 (1)	40.5	55	2.3	2.2	
T_2/ 4 h at 982°C	intercolony γ (3)	47.7	48.4	1.5	2.4	
	intercolony α_2 (4)	35[b]	61	1.7	2.3	
T_2/ 2 h at 900°C + aged 5040 h at 800°C	lamellar γ (6)[a]	47	48.3	1.7	3.0	
	lamellar α_2 (6)	31.7	64.5	1.5	2.3	
	intercolony γ (4)	47.6	47.7	1.8	3.0	
	intercolony α_2 (4)	31.3	65	1.5	2.2	
		P/M Ti-47Al-2Cr-1Nb-1Ta				
T_2/ 2 h at 900°C	lamellar γ (4)[a]	51.6	45.1	1.3	0.8	1.2
	lamellar α_2 (4)	39.5	55.4	2.5	0.8	1.8
	intercolony γ (2)	48.7	47.4	1.3	1.1	1.6
	intercolony α_2 (2)	38.6	56.5	2.3	1.1	1.7
T_2/ 4 h at 982°C	intercolony γ (2)	48.4	47.5	1.4	1.1	1.6
	intercolony α_2 (2)	33.6	61.2	1.5	0.8	1.9

a - number of individual measurements included in average
b - ± 3.6, which is a typical variation for individual measurements

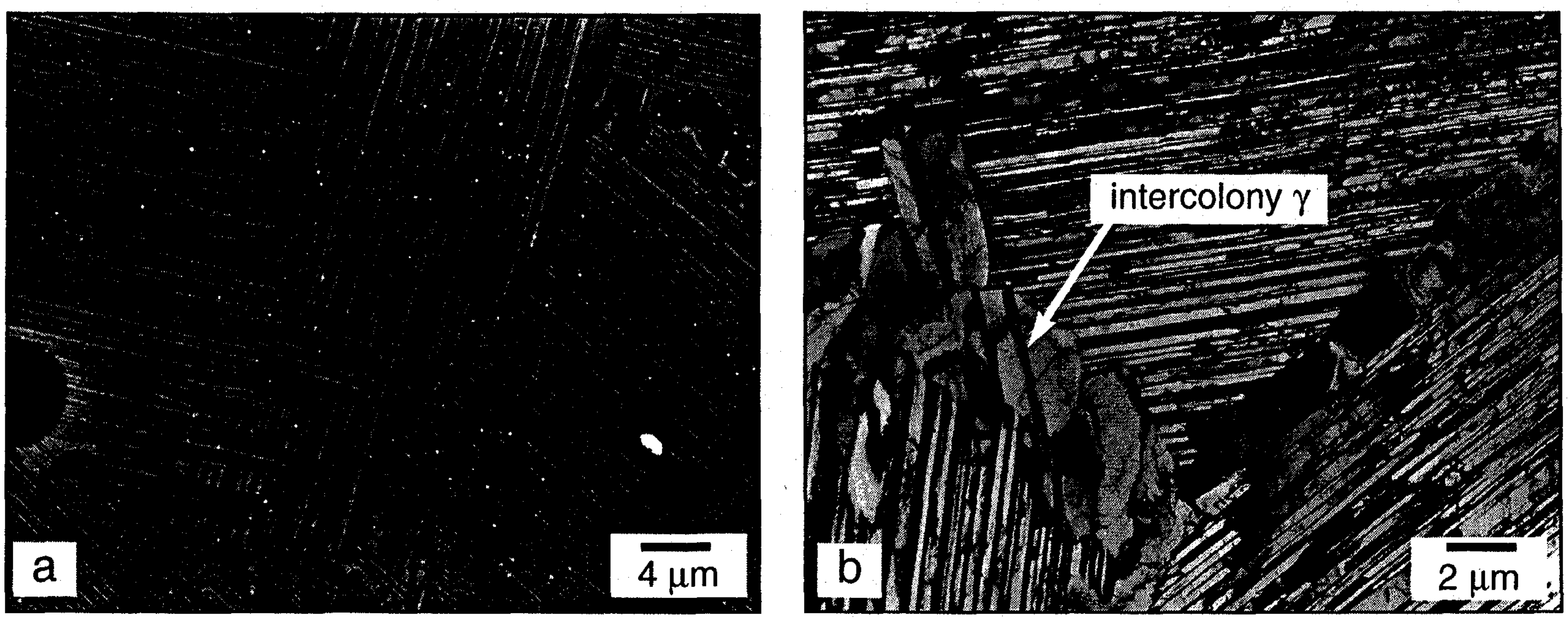

Fig. 1

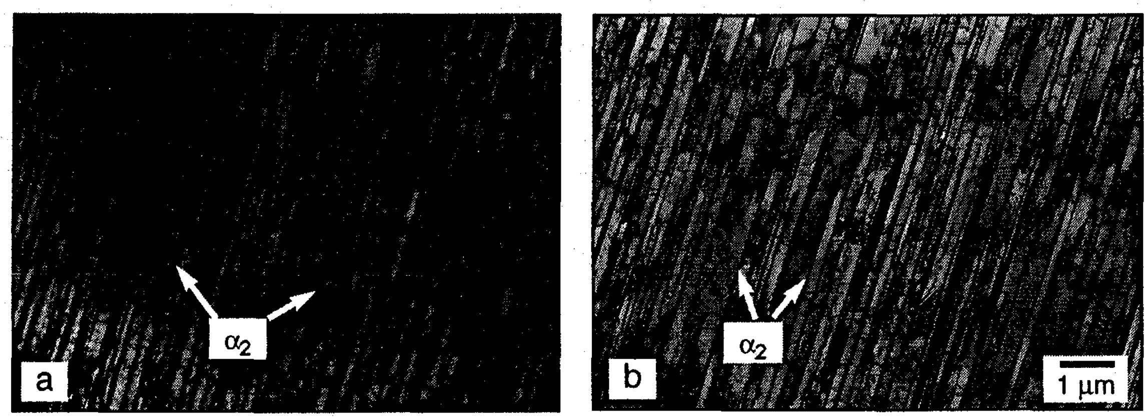

Fig. 2

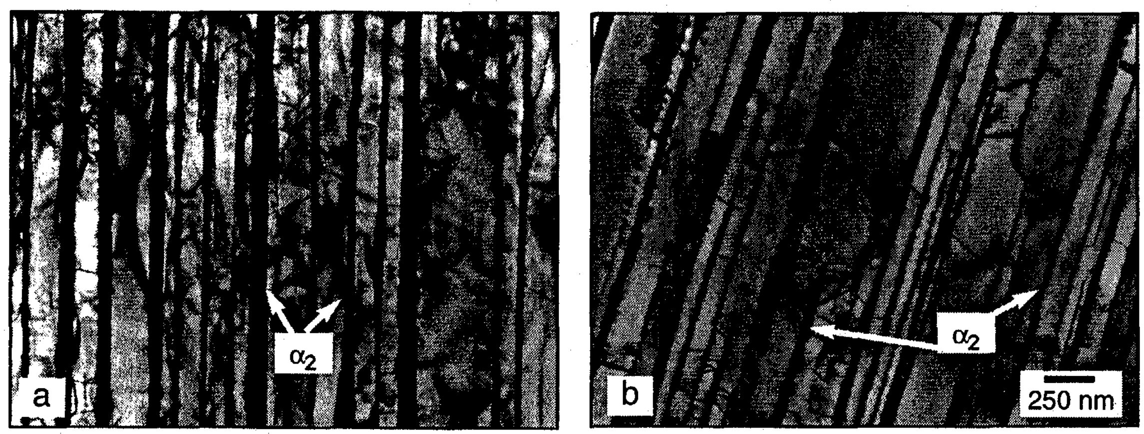

Fig. 3

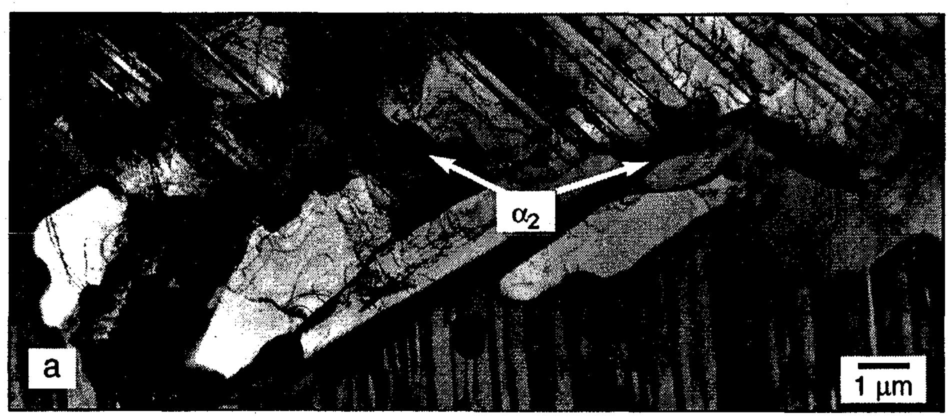

fig. 4

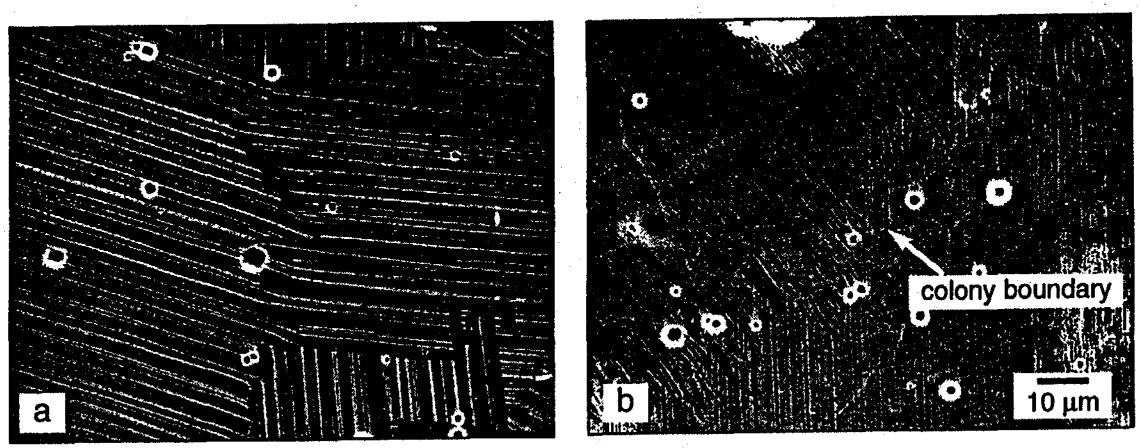

Fig. 5

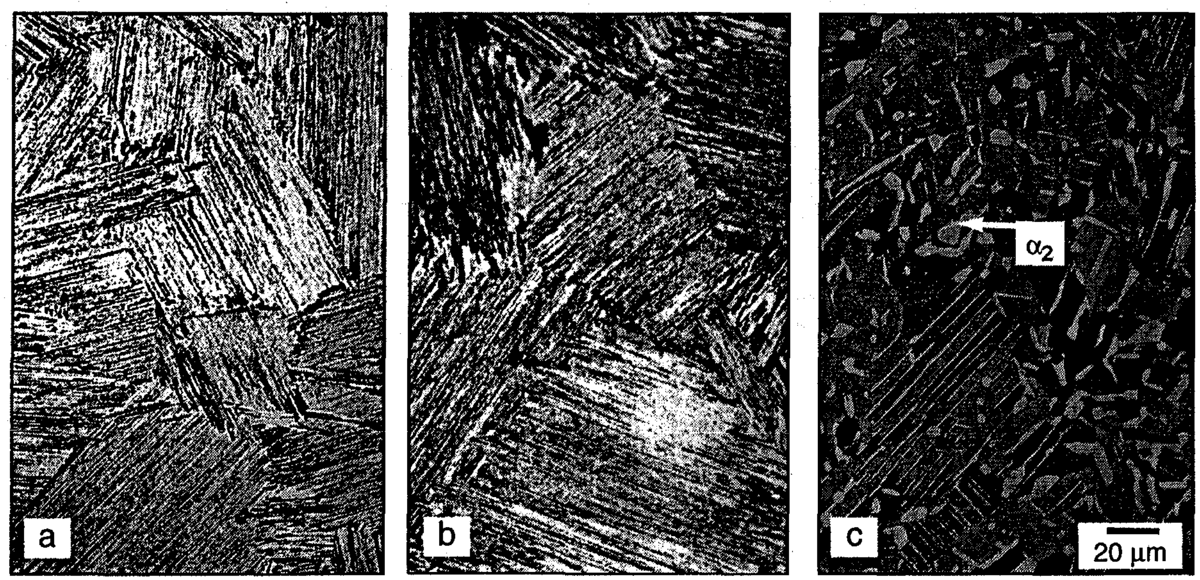

Fig 6

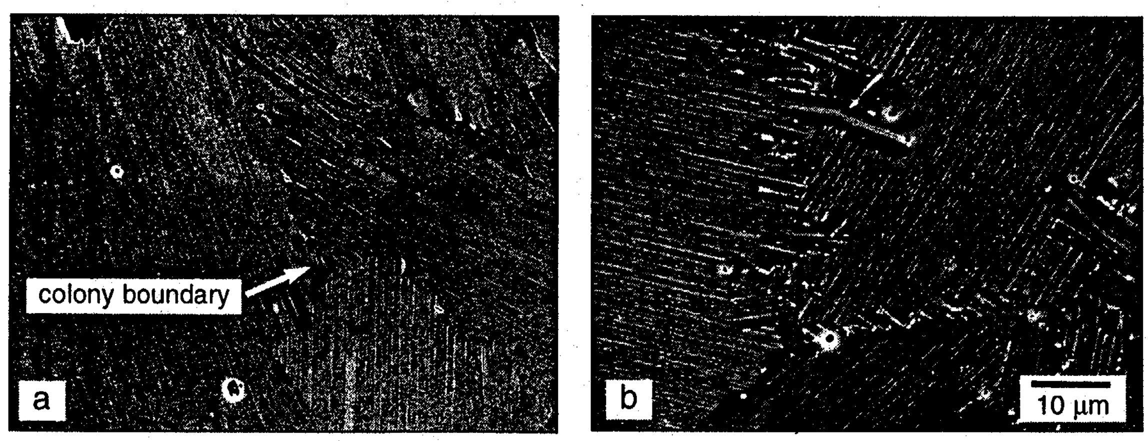

Fig. 7

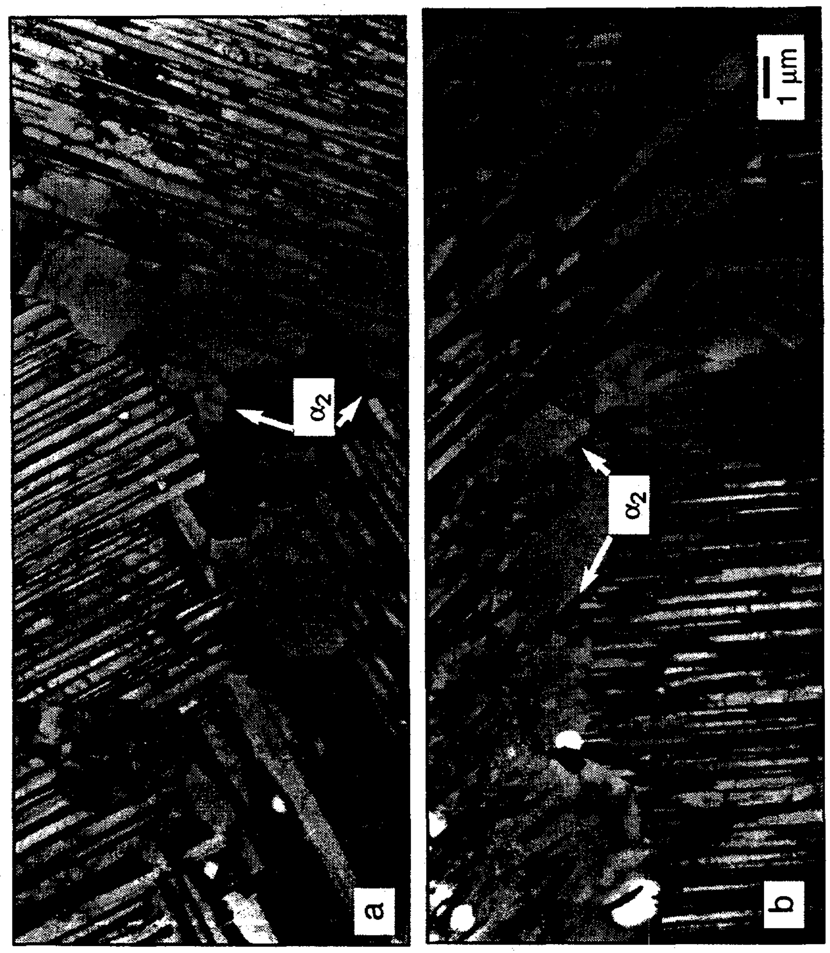

Fig. 8

DISCLAIMER